DOI: 10.1002/chem.200701868

Photoinduced Intramolecular Charge Transfer and S_2 Fluorescence in Thiophene-π-Conjugated Donor–Acceptor Systems: Experimental and TDDFT Studies**

Guang-Jiu Zhao,[a] Rui-Kui Chen,[b] Meng-Tao Sun,[c] Jian-Yong Liu,[a] Guang-Yue Li,[a] Yun-Ling Gao,[a] Ke-Li Han,*[a] Xi-Chuan Yang,*[b] and Licheng Sun*[b, d]

Abstract: Experimental and theoretical methods were used to study newly synthesized thiophene-π-conjugated donor–acceptor compounds, which were found to exhibit efficient intramolecular charge-transfer emission in polar solvents with relatively large Stokes shifts and strong solvatochromism. To gain insight into the solvatochromic behavior of these compounds, the dependence of the spectra on solvent polarity was studied on the basis of Lippert–Mataga models. We found that intramolecular charge transfer in these donor–acceptor systems is significantly dependent on the electron-withdrawing substituents at the thienyl 2-position. The dependence of the absorption and emission spectra of these compounds in methanol on the concentration of trifluoroacetic acid was used to confirm intramolecular charge-transfer emission. Moreover, the calculated absorption and emission energies, which are in accordance with the experimental values, suggested that fluorescence can be emitted from different geometric conformations. In addition, a novel S_2 fluorescence phenomenon for some of these compounds was also be observed. The fluorescence excitation spectra were used to confirm the S_2 fluorescence. We demonstrate that S_2 fluorescence can be explained by the calculated energy gap between the S_2 and S_1 states of these molecules. Furthermore, nonlinear optical behavior of the thiophene-π-conjugated compound with diethylcyanomethylphosphonate substituents was predicted in theory.

Keywords: charge transfer · density functional calculations · donor–acceptor systems · fluorescence · nonlinear optics

Introduction

Since the first observation by Lippert et al.,[1] the phenomenon of dual fluorescence for 4-(*N*,*N*-dimethylamino)benzonitrile (DMABN), one of the donor–acceptor π-conjugated (D-π-A) compounds, has led to numerous theoretical and experimental studies to explore the origin of intramolecular charge-transfer (ICT) fluorescence,[2–4] which plays a key

[a] G.-J. Zhao,+ Dr. J.-T. Liu, G.-Y. Li, Dr. Y.-L. Gao, Prof. Dr. K.-L. Han
State Key Laboratory of Molecular Reaction Dynamics
Dalian Institute of Chemical Physics
Chinese Academy of Sciences
457 Zhongshan Road, Dalian 116023 (China)
Fax: (+86) 411-84675584
E-mail: gjzhao@dicp.ac.cn
klhan@dicp.ac.cn

[b] R.-K. Chen,+ Dr. X.-C. Yang, Prof. Dr. L. Sun
State Key Laboratory of Fine Chemicals
Dalian University of Technology
158 Zhongshan Road, Dalian 116012 (China)
Fax: (+86) 411-83702185
E-mail: yangxc@dlut.edu.cn
lichengs@kth.se

[c] Dr. M.-T. Sun
National Laboratory for Condensed State Matter Physics
Institute of Physics, Chinese Academy of Sciences
P. O. Box 603-146, Beijing 100080 (China)

[d] Prof. Dr. L. Sun
KTH Chemistry, Organic Chemistry
Royal Institute of Technology
10044 Stockholm (Sweden)
Fax: (+46) 8-7908127

[+] These authors contributed equally to this work.

[**] TDDFT = Time-dependent density functional theory.

role in the photophysics of D-π-A compounds. After the finding of the importance of photoinduced ICT processes in biological systems such as photosynthesis,[5] interest in molecular donor–acceptor systems has increased significantly.[6–14] For several years, the dual-fluorescence properties of donor–acceptor systems have been used for studying molecular switches.[15–19] It was found that changes in molecular structure and conjugated system can induce very different optical and physical properties in D-π-A compounds.[20–51]

We have reported on the design, synthesis, and photophysical properties of a series for thiophene-π-conjugated D-π-A compounds culminating in 1-cyano-2-{5-[2-(1,2,2,4-tetramethyl-1,2,3,4-tetrahydroquinolin-6-yl)vinyl]thiophen-2-yl}vinylphosphonic acid diethyl ester (**QTCP**, Scheme 1).[52] In electronic spectral studies, **QTCP** was found to exhibit efficient ICT emission in polar solvents with large Stokes shift and strong solvatochromism.[52] Two main models have been proposed to explain the mechanism of formation of the intramolecular charge-transfer state: twisted intramolecular charge transfer (TICT) and planar intramolecular charge transfer (PICT).[4] In our previous investigations, detailed evidence on the ICT state revealed that, in the electronically excited state, charge transfer from the donor moiety (TMTHQ) to the electron-withdrawing species is accompanied by an anomalous 90° twist of the donor compound (TMTHQ) relative to the thiophene π bridge.[52] Hence, our results confirm the TICT model. Furthermore, these studies have revealed that the thiophene bridge is an ideal building block for construction of D-π-A compounds with ICT properties.[53]

It is well known that different substituents in electron-donor and -acceptor moieties will affect the electron distribution in the whole molecule and thus result in different photophysical and photochemical properties.[20,25–27] The π-conjugated bridge that connects the electron donor with the acceptor also influences the integrated characteristics.[25,27] Compounds containing a thiophene ring have been widely investigated with the aim of developing various optoelectronic devices such as organic light-emitting diodes (OLEDs), nonlinear optics (NLO), and dye-sensitized solar cells (DSSCs).[54–59] Since thiophene has a lower delocalization energy than benzene, it can offer better effective conjugation than benzene in donor–acceptor compounds.[59] To get a better understanding of the influence of different substituents on intramolecular charge transfer (ICT), we have now synthesized and fully characterized several derivatives of 1,2,2,4-tetramethyl-1,2,3,4-tetrahydroquinoline (TMTHQ) with different electron acceptors and thiophene π bridges. For comparison, benzene-bridged analogue **QBCP** (see Scheme 1) was also studied.

We first investigated the TMTHQ systems using steady-state absorption and fluorescence spectroscopy. Differences in absorption and fluorescence spectra for **QT**, **QTC**, **QTCP**, and **QBCP** in various solvents are discussed in detail. The fluorescence excitation spectra were also recorded to confirm the novel S_2 fluorescence phenomenon. Subsequently, the influence of adding of trifluoroacetic acid (TFA) to solutions of TMTHQs on their absorption and emission spectra were investigated. For better interpretation of our experimental results, the excited states of all the TMTHQ compounds considered were studied by time-dependent density functional theory (TDDFT).

Results and Discussion

Absorption spectra: Typical UV/Vis absorption spectra of **QT**, **QTC**, **QTCP**, and **QBCP** in different solvents at room temperature are shown in Figure 1. The strong absorption maximum in the visible region and relatively weak absorption peak in the near UV region correspond to the $S_1 \leftarrow S_0$ and $S_2 \leftarrow S_0$ electronic transitions, respectively. Moreover, all compounds in different solvents display intense and wide absorption bands. In general, an electron-withdrawing substituent at the thienyl 2-position can induce a remarkable red shift of the absorption maximum, the origin of which can be attributed to the ICT state for a strong push–pull system.[4–7] The broad absorption band can be assigned to electronic transitions delocalized throughout the whole molecule.[4] The thienylethyl and benzene π-bridging units en-

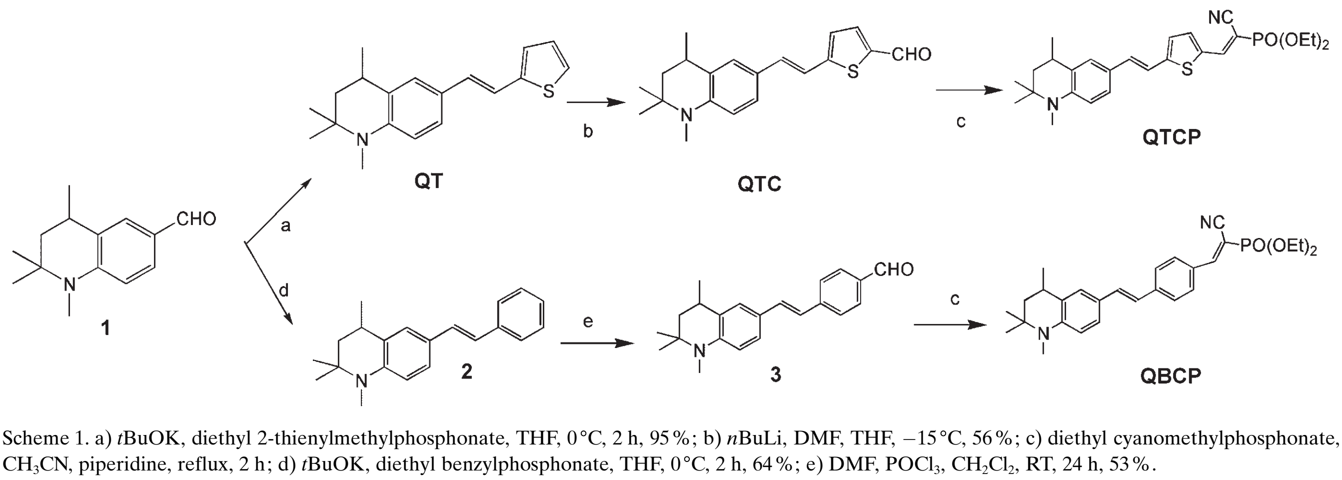

Scheme 1. a) *t*BuOK, diethyl 2-thienylmethylphosphonate, THF, 0 °C, 2 h, 95 %; b) *n*BuLi, DMF, THF, −15 °C, 56 %; c) diethyl cyanomethylphosphonate, CH_3CN, piperidine, reflux, 2 h; d) *t*BuOK, diethyl benzylphosphonate, THF, 0 °C, 2 h, 64 %; e) DMF, $POCl_3$, CH_2Cl_2, RT, 24 h, 53 %.

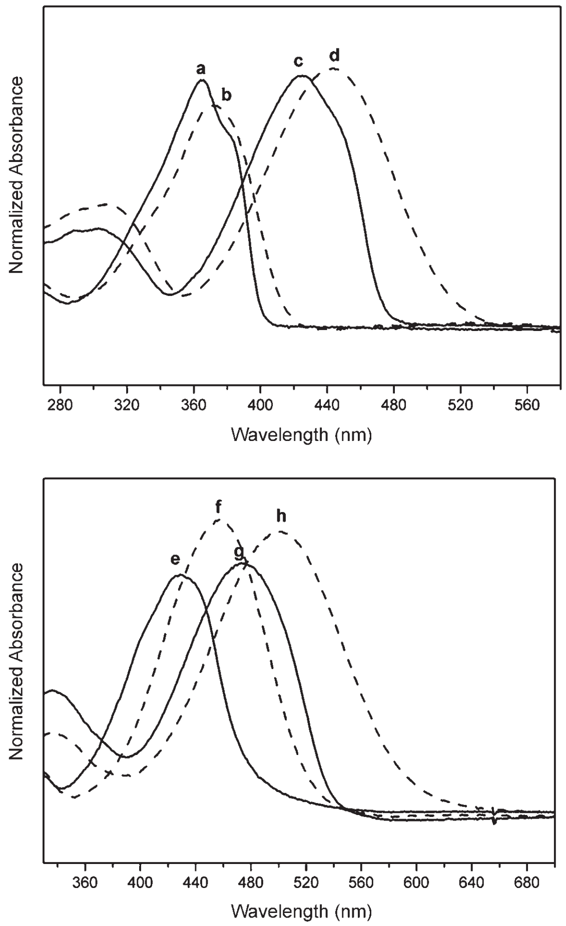

Figure 1. UV/Vis absorption spectra of **QT** (a, b), **QTC** (c, d), **QBCP** (e, f), and **QTCP** (g, h) in hexane (solid curves) and in acetonitrile (dashed curves).

large the conjugated system, so the absorption bands of **QTC**, **QTCP**, and **QBCP** are slightly broader than that of **QT**. In addition, the solvatochromic shift is rather small for **QT** (365 nm in hexane and 370 nm in acetonitrile). This indicates that the difference in dipole moments of the Franck–Condon (FC) excited state and the ground state of **QT** is quite small.[5] However, the solvatochromic shifts of **QTC**, **QTCP**, and **QBCP** are larger due to the larger difference in dipole moment of the FC excited state and the ground state, which is induced by the electron-withdrawing formyl and diethylcyanomethylphosphonate substituents.

Fluorescence spectra: The fluorescence spectra of all compounds exhibit fine structure in hexane but become structureless in diethyl ether and in more polar solvents (see Figure 2). In addition, unlike the absorption spectra, the fluorescence spectra of **QTC** and **QTCP** exhibit significant redshifts in polar solvents, indicative of a pronounced ICT characteristic of the fluorescent states.[52] As in the case of **QT**, the maxima of the emission spectra extend from 402 nm in hexane to 464 nm in MeCN, that is, a comparatively small solvatochromic shift of 62 nm. With an electron-withdrawing formyl substituent in the thienyl 2-position, the emission maxima of **QTC** range widely from 474 nm (in hexane) to 666 nm (in methanol), and the solvatochromic shift of **QTCP** becomes even as large as 224 nm on changing from hexane to methanol. This indicates that the magnitude of the solvatochromic shift also depends on the electron-withdrawing substituent at the thienyl 2-position in thiophene-π-conjugated TMTHQs. The smaller solvatochromic shift of **QBCP** with **QTCP** confirms that a thiophene bridge can offer more effective conjugation than a benzene bridge in donor–acceptor compounds.[59] Figure 2 shows that solvent polarity plays an important role in the fluorescence of **QTC** and **QTCP** in solution. In the fluorescent state, polar solvents can induce ICT, which is followed by geometric twisting.[52] Thus, fluorescence is emitted from the TICT state in polar solvents.[4,52] In addition, the fluorescence of **QTC** and **QTCP** in nonpolar solvents is emitted from the fluorescent states with planar conformations.[52]

S_2 fluorescence: Detailed absorption and fluorescence spectra of **QTCP** at different excitation wavelengths (Figure 3) clearly show the fine structure of the electronic transitions.

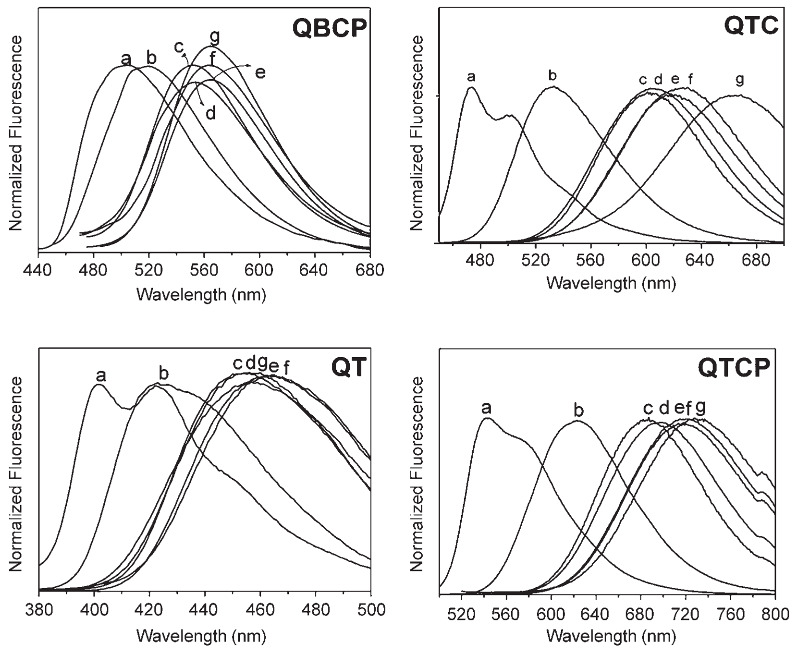

Figure 2. Normalized fluorescence spectra in a) hexane, b) diethyl ether, c) dichloromethane, d) acetone, e) DMF, f) acetonitrile, and g) methanol.

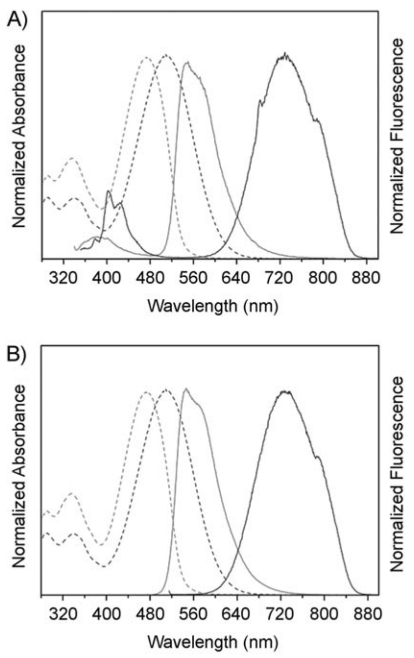

Figure 3. Normalized UV/Vis absorption (dashed lines) and emission spectra (solid lines) of **QTCP** in hexane (black) and methanol (gray). The emission spectra were recorded after excitation at 330 nm (A) and at the longest absorbance wavelength (B).

In addition to the strong absorption maxima in the visible region, a relatively weak absorption peak in the UV region can also be seen. The strong absorption peak corresponds to the $S_1 \leftarrow S_0$ electronic transition, and the relatively weak peak to the $S_2 \leftarrow S_0$ electronic transition. The two absorption bands, which are well resolved, may be due to the large energy gap between the S_2 and S_1 states.[31–38,59] Moreover, the weak peak has a smaller solvatochromic shift than the absorption maximum in more polar solvents. The weak peak is located at 336 nm in hexane and at 345 nm in methanol, while the absorption maximum is at 473 and 510 nm in hexane and methanol, respectively. Thus, compared with **QTCP** in hexane, the energy gap between the S_2 and S_1 states is larger in methanol because of better stabilization of the S_1 state in polar solvents.[4] This suggests that the S_1 state is more polar than the S_2 state due to the ICT character of the S_1 state.

The fluorescence spectra for excitation at different wavelengths corresponding to the $S_1 \leftarrow S_0$ and $S_2 \leftarrow S_0$ electronic transitions, respectively, are also shown in Figure 3. A novel feature was found in the fluorescence spectrum of **QTCP** after photoexcitation at 336 nm. In addition to the $S_1 \rightarrow S_0$ emission band, we also observed the appearance of a new emission band of low intensity on the blue side of the $S_1 \leftarrow S_0$ absorption band. Thus, we relate the origin of the new emission band to the $S_2 \rightarrow S_0$ fluorescence.[37,59] The Stokes shift of the S_1 state in polar solvents is larger than that of the S_2 state, and this could indicate ICT character for the S_1 state and LE nature for the S_2 state.[4] The energy gap between the S_2 and S_1 fluorescence states is significantly larger in polar solvents than in nonpolar solvents.

To confirm S_2 fluorescence, fluorescence excitation spectra for the two fluorescence peaks of **QTCP** were recorded (Figure 4). The fluorescence excitation spectra for the long-wavelength fluorescence of **QTCP** in both hexane and methanol are similar to the corresponding absorption spectra, in which the $S_1 \leftarrow S_0$ electronic transition band is much stronger than the $S_2 \leftarrow S_0$ transition band. However, only the $S_2 \leftarrow S_0$ electronic transition band can be observed in the fluorescence excitation spectra for the short-wavelength fluorescence, since the energy of $S_1 \leftarrow S_0$ electronic transition is lower than that of the short-wavelength fluorescence. The short-wavelength fluorescence can only originate from the S_2 state. Thus, the S_2 fluorescence of **QTCP** is confirmed by the fluorescence excitation spectra.

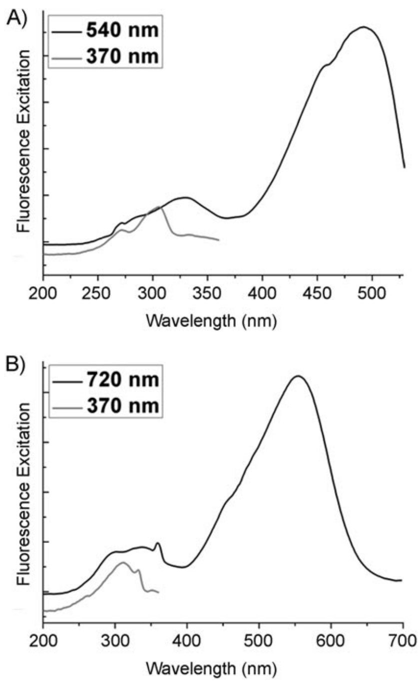

Figure 4. Fluorescence excitation spectra for S_1 fluorescence (black) and S_2 fluorescence (gray) of **QTCP** in hexane (A) and methanol (B).

Figure 5 shows the fluorescence emission spectra of **QT** and **QTC** for excitation at the wavelength corresponding to the $S_2 \leftarrow S_0$ transition. Only the S_1 fluorescence can be observed for **QT** and **QTC** in both hexane and methanol. This may be ascribed to the small energy gap between the S_2 and S_1 states, which facilitates nonradiative transition from the S_2 state to the S_1 state. Thus, S_2 fluorescence of **QT** and **QTC** molecules is not found.

The fluorescence emission and excitation spectra of **QBCP** in hexane and methanol are shown in Figure 6. In the fluorescence emission spectra with excitation at the S_1 absorption wavelength, only the S_1 fluorescence peak is observed in both hexane and methanol. When **QBCP** in hexane is excited at the S_2 absorption wavelength, both S_1

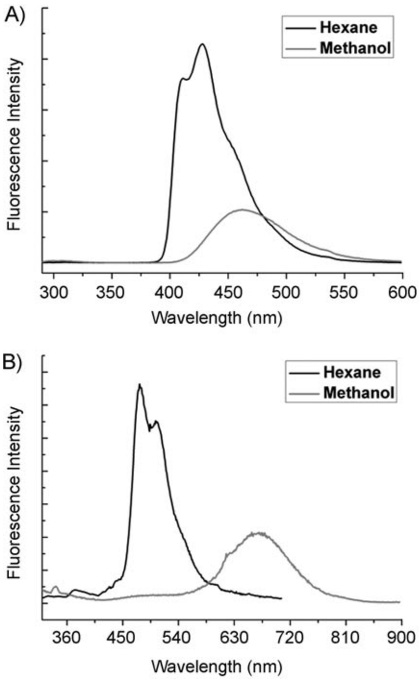

Figure 5. Fluorescence emission spectra with excitation at the wavelength corresponding to the S_2 absorption band. A) **QT**: 270 nm excitation; B) **QTC**: 310 nm excitation.

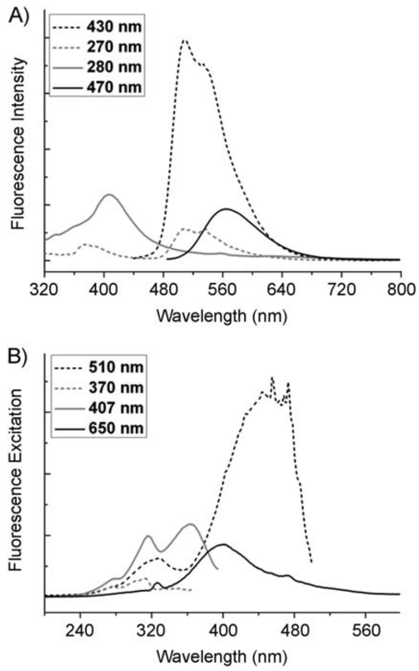

Figure 6. A) Fluorescence emission spectra with excitation at the wavelength corresponding to the S_1 and S_2 absorption bands for **QBCP** in hexane (dashed lines) and in methanol (solid lines). B) Fluorescence excitation spectra for S_1 fluorescence (black) and S_2 fluorescence (gray) of **QBCP** in hexane (dash lines) and methanol (solid lines).

and S_2 fluorescence is observed. Moreover, S_2 fluorescence is increased and comparable to S_1 fluorescence. Only the relatively strong S_2 fluorescence peak can be found in the fluorescence emission spectra of **QBCP** in methanol. It can be suggested that the energy gap between S_2 and S_1 states of **QBCP** is larger than that of **QTCP**. Furthermore, the S_2 fluorescence of **QBCP** is also confirmed by the fluorescence excitation spectra shown in Figure 6B.

Lippert–Mataga analysis: The photophysical properties of all compounds in various solvents are listed in Table 1. The Stokes shifts of all compounds are strongly dependent on both the electron-withdrawing substituents at the thienyl 2-position and the π-bridge substituents. The Stokes shifts of **QTC** and **QTCP** in polar solvents are significantly larger than those of **QT** and **QBCP** in the corresponding solvents. Moreover, the Stokes shifts of **QTC** and **QTCP** increase drastically with increasing the polarity of the solvents, while those of **QT** and **QBCP** depend only slightly on the solvent. The large Stokes shift can be ascribed to the ICT characteristics of the fluorescent states of **QTC** and **QTCP**. The magnitudes of the shifts from hexane to methanol are in the order of **QTCP** > **QTC** > **QBCP** > **QT**, which roughly parallels the relative electron-withdrawing ability of the substituents.[4,20] By using Φ_f and τ_f values, radiative ($k_r = \Phi_f/\tau_f$) and nonradiative ($k_{nr} = (1-\Phi_f)/\tau_f$) rates were calculated. The Φ_f

Table 1. Absorption (λ_{ab} [nm]) and emission (λ_{em} [nm]) maxima, Stokes shifts ($\Delta\lambda_{st}$ [nm]), fluorescence quantum yield (Φ_f) and lifetimes (τ_f [ns]), radiative (k_r [10^7 s^{-1}]), and nonradiative (k_{nr} [10^7 s^{-1}]) rates for all compounds in different solvents.

	Solv	λ_{ab}	λ_{em}	$\Delta\lambda_{st}$	Φ_f	τ_f	k_r	k_{nr}
	hexane	366	402	36	0.211	3.7	5.70	21.3
	Et_2O	368	423	55	0.171	3.9	4.38	21.3
	CH_2Cl_2	375	454	79	0.126	5.0	2.52	17.5
QT	acetone	372	454	82	0.137	4.3	3.19	20.1
	DMF	376	462	86	0.032	5.1	0.63	19.0
	MeCN	371	464	93	0.104	4.4	2.36	20.4
	MeOH	368	457	89	0.090	4.8	1.88	19.0
	hexane	473	544	71	0.144	3.2	4.50	26.8
	Et_2O	486	623	137	0.249	3.6	6.92	20.9
	CH_2Cl_2	509	687	178	0.181	6.3	2.87	13.0
QTCP	acetone	500	697	197	0.099	5.3	1.87	17.0
	DMF	511	718	207	0.048	4.3	1.12	22.1
	MeCN	500	721	221	0.050	3.9	1.28	24.4
	MeOH	510	734	224	0.022	2.8	0.79	34.9
	Solv	λ_{ab}	λ_{em}	$\Delta\lambda_{st}$	Φ_f	τ_2	k_r	k_{nr}
	hexane	425	474	49	0.066	3.4	1.94	27.5
	Et_2O	432	533	101	0.069	3.2	2.16	29.1
	CH_2Cl_2	453	601	148	0.143	3.2	4.47	26.8
QTC	acetone	442	603	161	0.160	3.5	4.57	24.0
	DMF	449	618	169	0.142	3.4	4.18	25.2
	MeCN	444	627	183	0.146	3.5	4.17	24.4
	MeOH	448	666	218	0.015	2.8	0.54	35.2
	hexane	429	505	76	0.224	5.4	4.15	14.4
	Et_2O	439	519	80	0.276	3.3	8.36	21.9
	CH_2Cl_2	462	552	90	0.064	3.1	2.06	30.2
QBCP	acetone	454	553	99	0.012	3.3	0.36	29.9
	DMF	463	564	101	0.008	3.3	0.24	30.1
	MeCN	457	563	106	0.007	3.0	0.23	33.1
	MeOH	471	565	94	0.001	2.9	0.03	34.5

and k_r values show that the compounds are less fluorescent in more polar solvents, especially in alcoholic solvents. Moreover, the nonradiative rate is correspondingly increased. Thus, nonradiative ICT process of the compounds can be facilitated by more polar solvents, especially protic alcoholic solvents, which can provide intermolecular hydrogen-bonding interactions.

The progressive increase of the Stokes shift with increasing solvent polarity can also be regarded as an indication of the increase in dipole moment from the ground state to the excited state.[20] To gain better insight into the solvatochromic behavior of all compounds, the spectral dependence on solvent polarity was studied on the basis of the Lippert–Mataga models,[68,69] (Figure 7). The dipole moment μ_e of

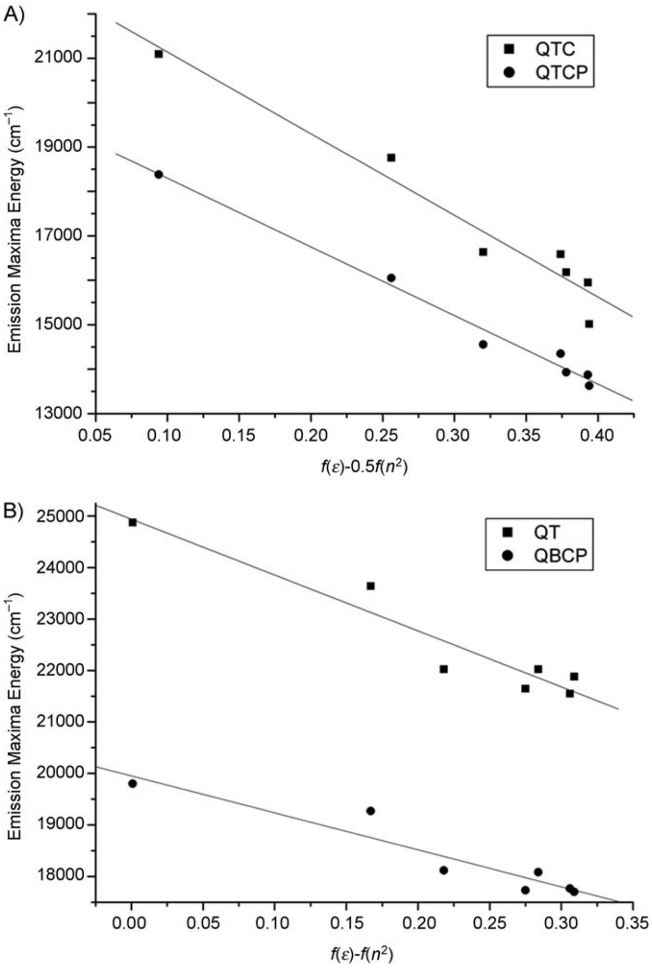

Figure 7. Correlation diagram of the energies of the fluorescence maxima against the Lippert–Mataga solvent parameter $f(\varepsilon,n)$.

the fluorescent state can be estimated from the slope m_f of the plot of the energy of the fluorescence maxima ν_f against the solvent parameter $f(\varepsilon,n)$ [Eqs. (1)–(4)].

$$\nu_f = -[(1/4\pi\varepsilon_0)(2hca^3)][\mu_e(\mu_e-\mu_g)]f(\varepsilon,n) + \text{Const.} \quad (1)$$

$$f(\varepsilon) = (\varepsilon-1)/(2\varepsilon+1) \quad (2)$$

$$f(n^2) = (n^2-1)/(2n^2+1) \quad (3)$$

$$a = (3m/4N\pi d)^{1/3} \quad (4)$$

where ε is the dielectric constant, n the refractive index, and a the Onsager radius of the solute, which can be derived from the Avogadro number N, molecular weight M, and density d. For an LE state, the applicable polarity function $f(\varepsilon,n)$ is $f(\varepsilon)-f(n^2)$, whereas $f(\varepsilon,n)=f(\varepsilon)-0.5f(n^2)$ is used for an ICT state. The dipole moments of the fluorescent state obtained by fitting Equation (1) and the values of some other parameters are listed in Table 2. The calculated dipole moments of the ground and fluorescence states are both in the order **QTCP** > **QTC** > **QBCP** > **QT**.

Table 2. Dipole moments of ground state and electronically excited states for **QT**, **QTC**, **QTCP**, and **QBCP**.

	a [Å][a]	m_f [cm^{-1}][b]	μ_g [D][c]	μ_e [D]
QT	4.90	−10856.2	3.99	8.32
QTC	5.05	−18397.7	10.14	21.2
QTCP	5.77	−15453.4	11.23	23.7
QBCP	5.74	−7188.8	10.03	17.2

[a] Onsager radius calculated by Equation (4) with d = 1.0 g cm^{-3} for **QT**, **QTC**, **QTCP**, and **QBCP**. [b] Calculated on the basis of Equation (1). [c] Calculated at the B3LYP/TZVP level.

Effect of added trifluoroacetic acid: The dependence of the absorption and emission spectra of thiophene-π-conjugated **QT**, **QTC**, and **QTCP** in methanol on the concentration of trifluoroacetic acid (TFA) was investigated (Figure 8). For all compounds, addition of TFA leads to disappearance of the original absorption bands and formation of a new band at shorter wavelength. The new absorption bands can be attributed to absorption of protonated forms of the compounds. Moreover, protonation at the amino group can eliminate the ICT process in these compounds, and the fluorescence process can then only occur from the protonated forms with planar structures.[70,71] Thus, fluorescence emission from the TICT fluorescence state of **QTC** and **QTCP** in polar solvents can disappear after they are completely protonated. The emission spectra were recorded after excitation around the maximum of the absorption spectra in the absence of TFA and excitation around the newly formed absorption band when TFA was added.

Generally, the emission spectra in the presence of TFA should have two bands corresponding to the protonated and nonprotonated forms.[70] In the case of **QT**, the emission spectra in the presence of TFA show only one emission band, whereby the two bands from the protonated and nonprotonated forms are not resolved. This confirms that the fluorescent state for **QT** is of LE character. However, there are two unambiguous bands for **QTC** and **QTCP** in methanol in the presence of TFA. The added TFA induces decreased intensity of the original emission bands and formation of new emission bands at higher frequency, which can

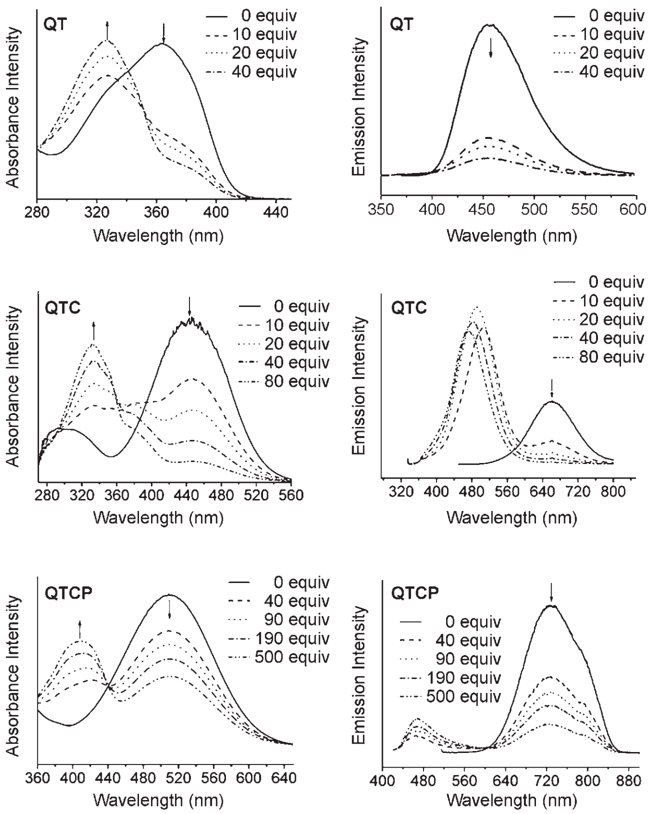

Figure 8. Effect of protonation on the absorption and emission spectra of **QT**, **QTC**, and **QTCP** in methanol at 297 K.

be assigned to the protonated form.[71] Since protonation at the amino group can lead to elimination of the charge-transfer process in the molecule,[70,71] the size of the emission shift from the nonprotonated form to the protonated form can be used to measure the ICT property of the fluorescent state. The shift of emission spectra for **QTC** in methanol due to protonation is as large as about 200 nm. However, the shift for **QTCP** in methanol is even larger (about 300 nm). Thus, **QTCP** in methanol shows better ICT character than **QTC**. In the presence of TFA, both **QTC** and **QTCP** in methanol exhibit decreases in ICT emission and new emissions from the protonated form. In addition, the newly formed emission bands for the protonated forms are significantly shifted with respect to the emission bands of the nonprotonated forms. This confirms the TICT nature of the original fluorescent states for **QTC** and **QTCP** in methanol before adding TFA. For **QT** in solution, however, the emission more likely originates from the LE state.

Optimized structures: Structures of ground and electronically excited states of all compounds in planar and twisted conformations were optimized. Some important bond lengths, bond angles, and dihedral angles in the optimized structures are listed in Table 3. The benzene and thiophene rings are nearly in a plane in all ground-state structures. The dihedral angles in the ground states reveal that electron-withdrawing groups make the molecules more planar. In addition, bonds 2 and 4 are slightly shortened after adding electron-withdrawing groups to **QT**, while bond 3 is lengthened. The most significant feature is the structural changes in electronically excited states compared to the ground state. In particular, bond 2 is slightly shortened in both S_1 and S_2 states for **QT** and **QBCP**. This bond is slightly lengthened in the S_1 state but slightly shortened in the S_2 state for **QTC** and **QTCP.** Bond 2 is significantly lengthened in the TICT states of **QTC** and **QTCP**. The molecular backbones of **QTC** and **QTCP** are less planar in the S_1 state than in the ground state according to the calculated dihedral angles. On the contrary, the backbones of **QTC** and **QTCP** are more planar in the S_2 state than in the ground state. Moreover, the structures of **QT** and **QBCP** in both S_1 and S_2 states are always more planar than in the ground state. Therefore, the less planar molecular backbones of **QTC** and **QTCP** in the S_1 state may indicate that ICT takes place in this state.

Molecular orbitals: Frontier molecular orbitals (MOs) are displayed in Figure 9 for the planar (all compounds) and twisted (only **QTC** and **QTCP**) conformations. According to

Table 3. Optimized structural parameters for **QT**, **QTC**, **QTCP**, and **QBCP** in different electronic states in planar and twisted conformations. L: bond lengths [Å]; A: bond angles [°]; DA: dihedral angles [°].

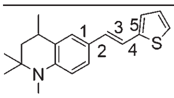	**QT**			**QTC**				**QTCP**				**QBCP**		
		planar			planar		twisted		planar		twisted		planar	
	GS	S_1	S_2	GS	S_1	S_2	TICT	GS	S_1	S_2	TICT	GS	S_1	S_2
L(1)	1.406	1.422	1.423	1.407	1.412	1.412	1.415	1.408	1.410	1.415	1.406	1.407	1.408	1.415
L(2)	1.456	1.425	1.424	1.451	1.452	1.442	1.499	1.449	1.454	1.436	1.485	1.452	1.462	1.438
L(3)	1.348	1.398	1.378	1.351	1.369	1.369	1.374	1.353	1.360	1.379	1.353	1.350	1.350	1.378
L(4)	1.447	1.404	1.421	1.442	1.426	1.412	1.435	1.439	1.436	1.417	1.428	1.454	1.464	1.435
L(5)	1.377	1.410	1.394	1.388	1.397	1.413	1.416	1.390	1.386	1.413	1.393	1.411	1.406	1.422
A(12)	119.2	120.1	117.6	119.2	119.5	119.4	121.2	119.2	119.4	119.5	121.3	119.2	118.9	119.2
A(23)	127.5	124.5	127.7	127.7	124.9	127.2	122.8	127.7	125.5	126.4	122.7	127.7	126.1	127.0
A(34)	125.5	124.8	125.6	125.0	126.9	125.8	128.8	124.9	126.7	124.2	128.3	126.7	127.5	125.8
A(45)	131.3	129.5	131.7	130.6	129.9	130.0	130.3	130.5	130.4	129.6	130.0	123.9	123.2	124.3
DA(123)	3.612	2.336	4.788	1.890	8.027	1.196	105.3	1.178	9.777	1.091	105.2	1.222	0.978	1.259
DA(345)	2.629	1.286	2.359	0.331	3.670	0.299	179.6	0.552	2.972	0.572	179.8	0.306	0.588	0.538

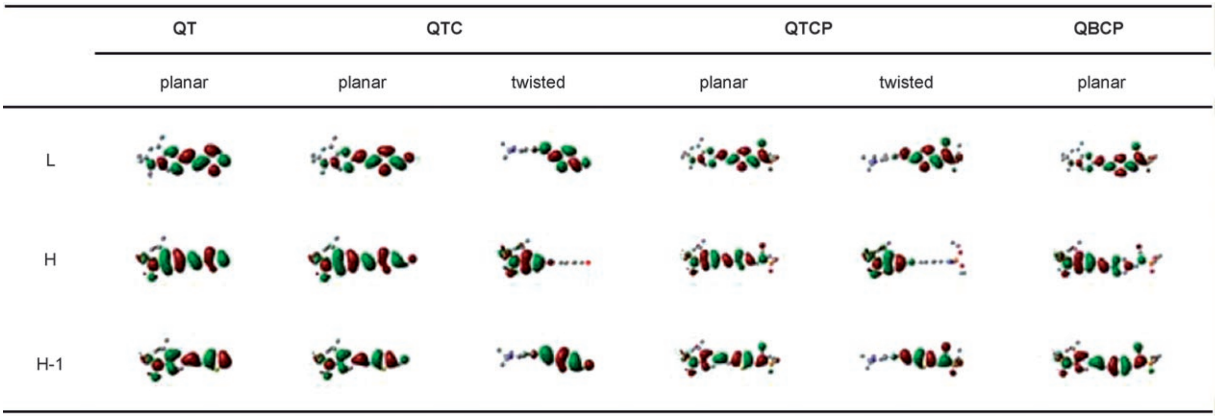

Figure 9. Frontier MOs for different species in planar and twisted conformations. H: HOMO; L: LUMO.

our TDDFT calculations, the S_1 state corresponds to the HOMO→LUMO transition, and the S_2 state to the HOMO−1→LUMO transition. Thus, only the HOMO−1, HOMO, and LUMO orbitals in the planar and twisted structures are shown here. For all the molecules in planar conformation the electron densities of all the orbitals shown here are delocalized over the whole molecule. This can contribute to broad absorption bands in the absorption spectra of all compounds. For the perpendicular geometric structures, the electron density of the HOMO is localized on the donor moiety, while the electron densities of both LUMO and HOMO−1 orbitals are only localized on the acceptor moiety. Thus, the ICT nature of the S_1 state and the LE character of S_2 state are demonstrated.

Density of states: The calculated total density of states (TDOS) and the projected density of states (PDOS) for **QTCP** in planar and twisted conformations are shown in Figure 10. The PDOS can provide insight into the roles of different fragments in the **QTCP** molecule.[72,73] The most significant feature of the DOS is that HOMO−1 has similar contributions of fragments to the LUMO, while the HOMO is very different from the LUMO. The main contributions to the HOMO−1 and LUMO come from the thiophene ring and cyano group, while the contributions from the benzene ring and the nitrogen atom of the donor are relatively small, especially in the twisted conformation. This suggests that the transition from HOMO−1 to LUMO is not followed by a drastic intramolecular charge redistribution between different fragments.[4] Thus, the S_2 state, which corresponds to the HOMO−1→LUMO transition, is an LE state. However, the benzene ring and nitrogen atom of the donor make the main contributions to the HOMO. Clearly, the transition from the HOMO to the LUMO can be followed by charge decrease on the benzene ring and nitrogen atom of the donor and charge increase on the thiophene ring and cyano group, so the ICT nature of the S_1 state is evident.

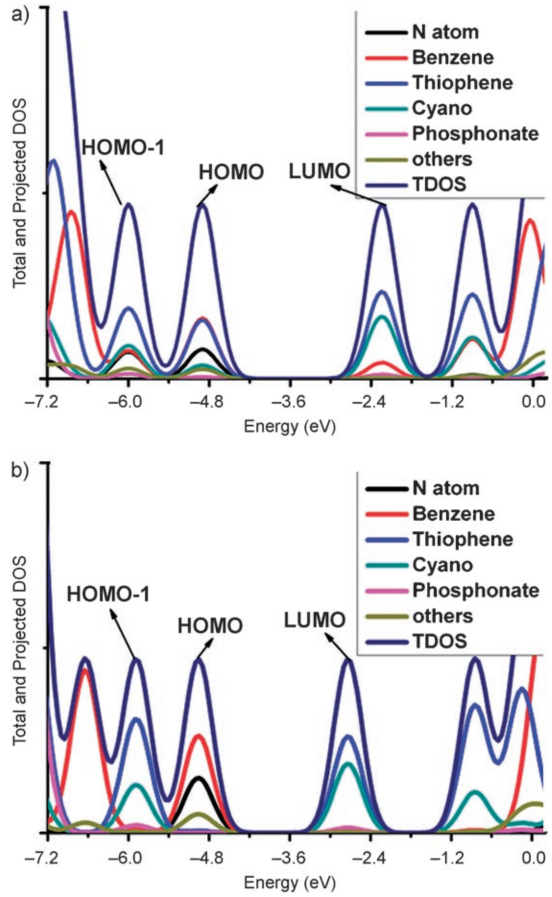

Figure 10. Total density of states (TDOS) and projected density of states (PDOS) for a) planar **QTCP** and b) twisted **QTCP**.

Calculated excitation energies and energy gap between S_2 and S_1 states: In Table 4, calculated and experimental absorption and fluorescence electronic excitation energies for all compounds in planar conformation and twisted **QTC** and **QTCP** are presented. All the calculated excitation energies coincide well with the experimental values. Comparison of the calculated and experimental S_1 fluorescence emission energies shows that the S_1 fluorescence of **QTC** and **QTCP** in nonpolar solvents is emitted from the excited states in the

Table 4. Calculated absorption and fluorescence electronic excitation energies [nm^{-1}] for all compounds and corresponding experimental values (in parentheses) in planar (in hexane) and twisted (in acetonitrile) conformations.

		QT	QTC		QTCP		QBCP
		planar	planar	twisted	planar	twisted	planar
Abs.	S_1	381 (366)	442 (425)	–	497 (473)	–	491 (429)
	S_2	309 (268)	352 (303)	–	363 (336)	–	343 (266)
	ΔE[a]	0.764	0.722	–	0.918	–	1.081
Flu.	S_1	425 (402)	462 (474)	587 (627)	521 (544)	701 (721)	518 (505)
	S_2	–	–	–	389 (383)	–	361(367)

[a] ΔE is the energy gap [eV] between the S_1 and S_2 states.

planar conformation, while in polar solvents (e.g. in acetonitrile) it is emitted from the ICT state in the twisted conformation.[4,52] Thus, the polarity of solvents plays an important role for S_1 fluorescence of **QTC** and **QTCP** in solution.[4] In the S_1 fluorescent state, the solvent polarity can induce ICT followed by geometric twisting,[52] while the fluorescence of **QT** and **QBCP** is emitted from the planar geometric structures, since no evident ICT process can occur. In addition, site-specific intermolecular hydrogen bonding interactions can also influence the electronic spectra, such as quenching fluorescence.[60–67]

As discussed above, the S_2 fluorescence can be observed for **QTCP** and **QBCP** but not for **QT** and **QTC**. This may be correlated with the energy gap between S_2 and S_1 states.[59] Thus, the calculated energy gaps between S_2 and S_1 states for all the compounds are also listed in Table 4. The calculated energy gap between S_2 and S_1 states of **QTCP** is as high as 0.918 eV. The large energy gap between S_2 and S_1 states can decrease the rate of the internal conversion from S_2 state to S_1 state as well as some other nonradiative processes.[59,63] So the S_2 state of **QTCP** molecule can emit fluorescence. The energy gaps of **QT** and **QTC** are very close and much smaller than that of **QTCP**. The small energy gap between S_2 and S_1 states increases the electronic coupling of the two electronically excited states, and thus facilitates internal conversion from the S_2 state to S_1 state.[59,63] Hence, the S_2 fluorescence for **QT** and **QTC** cannot be measured. The energy gap between the S_2 and S_1 states of **QBCP** is larger than that of **QTCP**; thus, **QBCP** has strong S_2 fluorescence.

Potential-energy curves: Potential-energy curves as a function of the twisting angle were calculated for the ground and low-lying excited states of all compounds (Figure 11). The potential-energy curves of **QTCP** are representative of TICT character.[44,45] In the ground state, **QTCP** prefers a planar structure, and the twisted structure is unstable. On photoexcitation, planar **QTCP** can be initially excited to the S_1 or S_2 state of planar geometry. The potential-energy curve of the S_1 state has a minimum at the perpendicular geometry. Generally, there is an energy barrier between the planar and perpendicular structures in the S_1 state.[44,45] Photoexcited **QTCP** in nonpolar solvents cannot pass through the energy barrier in the S_1 twisting-angle potential-energy curve and only emits fluorescence from the planar structures. However, polar solvents can decrease the energy barrier, and thus photoexcited **QTCP** can pass through the energy barrier easily.[44,45] Hence, S_1 fluorescence is preferably emitted from the perpendicular geometric structure for **QTCP** in polar solvents. According to the potential-energy curve of

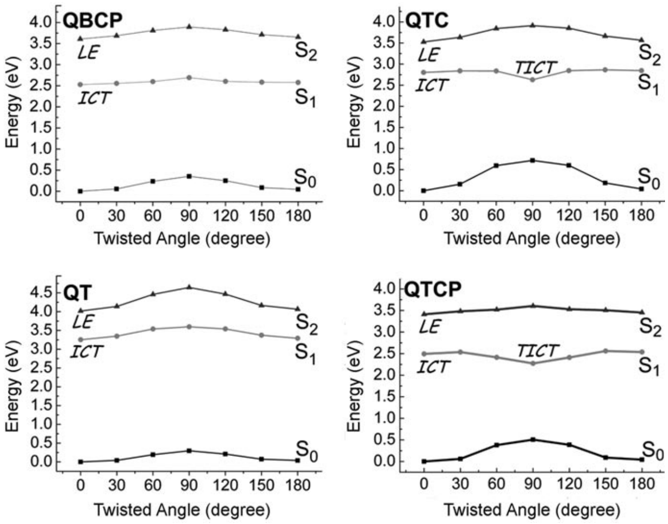

Figure 11. Calculated potential-energy curves as a function of twisting angle for different electronic states for all compounds.

QTCP, the fluorescence of the TICT state is drastically red-shifted, which is consistent with the experimental value. In contrast, the S_2 the twisting-angle potential-energy curve has a maximum at the perpendicular geometry, so S_2 fluorescence is preferably emitted from the planar geometry. The potential-energy curves of **QTC** are also of TICT character, while the energy gap between S_2 and S_1 states is smaller than that of **QTCP**. Thus, the S_2 fluorescence emission cannot be observed. However, the potential-energy curves of **QT** and **QBCP** differ from that of **QTCP** and **QTC**. Both **QT** and **QBCP** with perpendicular geometries are unstable in all electronic states. Hence, fluorescence of **QT** and **QBCP** can only be emitted from the planar conformations. Table 5

Effects of protonation: The **QT, QTC**, and **QTCP** molecules protonated at the nitrogen atom of the donor moiety were also investigated here and the results compared with experimental data. Protonation at the amino group can eliminate the ICT process of the compounds, and then fluorescence can only occur from the protonated forms with planar structure. Thus, only the planar conformations for the protonated **QT, QTC**, and **QTCP** molecules are presented here. The calculated electronic excitation energies and the oscillator

Table 5. Calculated absorption electronic excitation energies [nm] and corresponding oscillator strengths (in parentheses) for protonated compounds in the planar conformation.

	Protonated **QT**	Protonated **QTC**	Protonated **QTCP**
S_1	373 (0.966)	396 (0.000)	429 (1.520)
S_2	349 (0.065)	380 (1.209)	359 (0.020)
S_3	307 (0.015)	336 (0.030)	329 (0.127)
S_4	285 (0.009)	311 (0.015)	317 (0.006)
S_5	263 (0.102)	288 (0.082)	313 (0.053)

strengths for corresponding electronic states are listed in Table 5. The absorption maxima are located at 373, 380, and 429 nm for protonated **QT, QTC**, and **QTCP**, respectively. They are in good agreement with the new bands detected experimentally in the shorter wavelength region after adding TFA. Therefore, these bands are confirmed to be absorption bands of the protonated forms. The TDDFT results show that all the absorption maxima correspond to transitions from HOMO to LUMO. In the HOMO and LUMO of the protonated compounds (Figure 12), the LE character of the transition from HOMO to LUMO is distinctly evident.

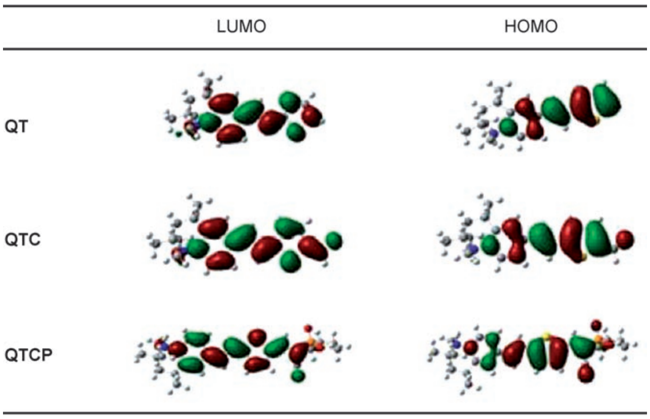

Figure 12. HOMO and LUMO for protonated compounds in planar conformation.

2D and 3D real-space analysis of QTCP: Transition energies and oscillator strengths were calculated with the TD-B3LYP method and the 6-31G(D,P) basis set by using the Gaussian 03 program suite. Transition density (TD) and charge difference density (CDD) for **QTCP** at the planar and twisted conformations are shown in Figure 13. The charge difference densities clearly reveal the result and orientation of ICT. The electron and hole populations of the S_1 state are well separated, that is, the electron can transfer from the nitrogen atom of the donor and benzene ring to the thiophene ring and the cyano group. This is accordance with our analysis above. The orientation and strength of the transition dipole moments of the excited states can be determined from the TDs. Moreover, the S_2 state has two transition dipole moments with opposite orientations ($\mu=\mu_a+\mu_b$). Given the relationship $|\mu|^2\sim f/E$,[75] the reason why the

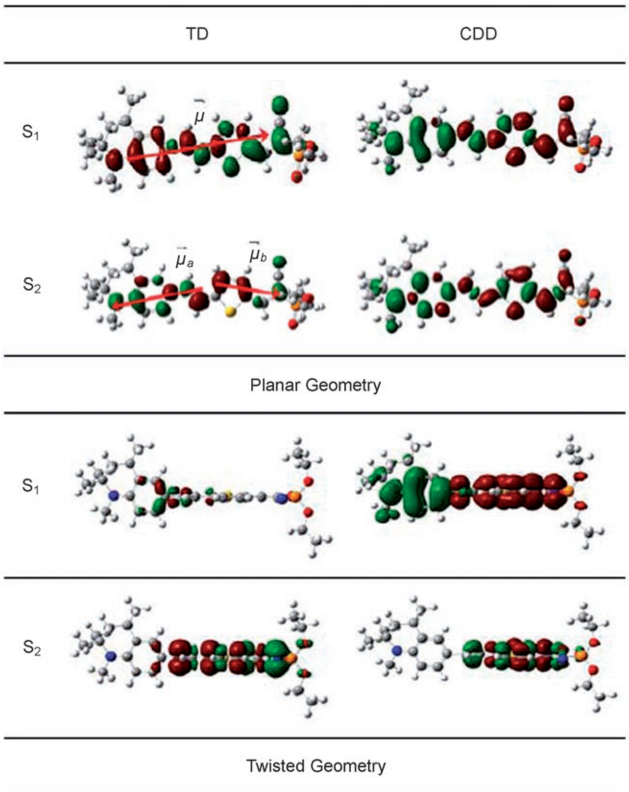

Figure 13. Transition density (TD) and charge difference density (CDD) of **QTCP** in planar and twisted conformations. Green and red stand for hole and electron, respectively. The isovalue is 4×10^{-4} a.u.

dipole moment of S_2 is smaller than that of S_1 can be easily understood.

Large changes in transition dipole moment and polarizability in the transition process may result in a nonlinear optical (NLO) response, which is very important for two-photon absorption in the donor–acceptor system.[76–78] They can be fitted by the static electric field dependent transition energy $E_{exc}(F)=E_{exc}(0)-\Delta\mu F-\Delta\alpha F^2/2$, where $E_{exc}(0)$ is the excitation energy at zero field F, $\Delta\mu$ the change in dipole moment, and $\Delta\alpha$ the change in polarizability.[78] According to the fitted results shown in Figure 14, for single-photon absorption, the absorption peak of S_1 should be larger than that of

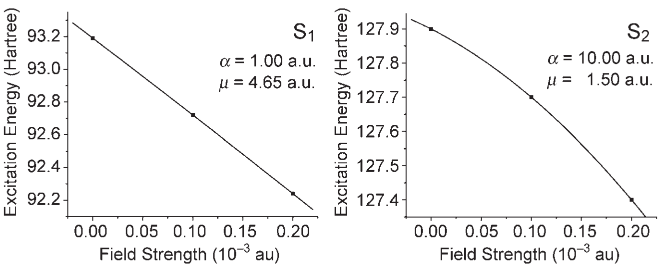

Figure 14. Excitation energy versus electric field strength for the S_1 and S_2 states. Insets show the fitted results.

S_2, since $\mu_1 > \mu_2$, and for two-photon absorption the peak of S_2 would be larger than S_1, since $\alpha_2 \gg \alpha_1$.[78]

Conclusion

The newly synthesized thiophene-π-conjugated D-π-A compounds **QT**, **QTC**, **QTCP**, and **QBCP** have been systematically investigated by experimental and theoretical methods. Both steady-state spectroscopic results and theoretical calculations show that the fluorescence emission of the thiophene-π-conjugated compounds is strongly dependent on the electron-withdrawing substituents at the thienyl 2-position. Compound **QTCP** can emit both S_1 and S_2 fluorescence. For **QTCP** in nonpolar solvents, S_1 fluorescence is emitted from the planar conformation, whereas S_1 fluorescence is emitted from the twisted ICT (TICT) state in the perpendicular conformation for **QTCP** in polar solvents. Furthermore, the TICT mechanism of **QTCP** in polar solvents has been demonstrated by various spectroscopic results and theoretical calculations. Compound **QTCP** can also emit S_2 fluorescence in both nonpolar and polar solvents in the planar conformation, and S_2 fluorescence was confirmed by the fluorescence excitation spectra. The S_1 fluorescence behavior of **QTC** in different solvents is similar to that of **QTCP**. However, no S_2 fluorescence can be observed for **QTC** in both nonpolar and polar solvents. Compound **QT** also exhibited no S_2 fluorescence in various solvents. Our theoretical calculations showed that the energy gaps between the S_2 and S_1 states for **QTC** and **QT** are markedly smaller than that of **QTCP**. The small energy gap between S_2 and S_1 states facilitates nonradiative deactivation of the S_2 state, and thus S_2 fluorescence is quenched. Moreover, our spectroscopic results show the absence of a TICT state for **QT** and **QBCP**. This was demonstrated by our calculated potential-energy curves of these compounds. Therefore, the S_1 fluorescence can only be emitted from the planar conformation for **QT** and **QBCP** in various solvents. Interestingly, strong S_2 fluorescence can be observed for **QBCP** in polar solvents. This is attributed to the larger energy gap between S_2 and S_1 states of **QBCP** compared to **QTCP**.

Experimental Section

^{1}H NMR spectra were obtained on a Varian INOVA 400 MHz NMR spectrometer. Mass spectra were recorded on a Q-TOF mass spectrometer (Micromass, England). The electronic absorption spectra were measured on a HP-8453 spectrophotometer. The fluorescence measurements were performed on a PTI-C-700 Felix and Time-Master system. The fluorescence quantum yields were determined by the relative method using optically matched solutions. Quinine sulfate in 1 N sulfuric acid (Φ_f = 0.546 at 25 °C) was used as standard. The accuracy of the quantum yields reported here is expected to be better than ±10%. Fluorescence lifetimes were determined on a chronos fluorescence lifetime spectrometer (ISS Champagn, IL, USA). Solvents were used as received for absorption and fluorescence spectral measurement.

The synthesis of the D-π-A compounds involved in the present work is shown in Scheme 1. Starting compound **1** was synthesized according to a literature procedure.[79,80] Wittig–Horner reactions of **1** and corresponding phosphonates gave **QT** and **2** in high yield. Introduction of the aldehyde group on the thiophene ring with by *n*BuLi and DMF provided **QTC**. Compound **3** was obtained by Vilsmeier reaction of **2**. Compounds **QTCP** and **QBCP** were synthesized by Knoevenagel condensation of the corresponding aldehydes with diethyl cyanomethylphosphonate and piperidine as catalyst. All intermediates and target compounds were characterized by ^{1}H NMR spectroscopy and HRMS.

QT: ^{1}H NMR ([D$_6$]acetone, 400 MHz): δ = 1.21 (s, 3 H), 1.30 (s, 3 H), 1.36 (d, J = 6.7 Hz, 3 H), 1.46 (dd, J_1 = 12.7 Hz, J_2 = 13.0 Hz, 1 H), 1.85 (dd, J_1 = 4.5 Hz, J_2 = 12.9 Hz, 1 H), 2.84 (s, 3 H), 2.80–2.87 (m, 1 H), 6.56 (d, J = 8.5 Hz, 1 H), 6.88 (d, J = 16.0 Hz, 1 H), 6.98–7.0 (m, 1 H), 7.04 (d, J = 3.5 Hz, 1 H), 7.15 (d, J = 16.1 Hz, 1 H), 7.23–7.24 (m, 2 H), 7.31 ppm (s, 1 H); HRMS-EI calcd for $C_{19}H_{23}NS$ [M]$^+$: 297.1551; found: 297.1546.

QTC: ^{1}H NMR ([D$_6$]acetone, 400 MHz): δ = 1.24 (s, 3 H), 1.32 (s, 3 H), 1.37 (d, J = 6.6 Hz, 3 H), 1.47 (dd, J_1 = 12.7 Hz, J_2 = 12.9 Hz, 1 H), 1.87 (dd, J_1 = 4.4 Hz, J_2 = 13.0 Hz, 1 H), 2.88 (s, 3 H), 2.79–2.85 (m, 1 H), 6.59 (d, J = 8.6 Hz, 1 H), 7.20–7.22 (m, 3 H), 7.33 (dd, J_1 = 1.7 Hz, J_2 = 8.5 Hz, 1 H), 7.39 (s, 1 H), 7.82 (d, J = 3.9 Hz, 1 H), 9.85 ppm (s, 1 H); HRMS-EI calcd for $C_{20}H_{23}NOS$: 325.1500 [M]$^+$; found: 325.1500.

QTCP: ^{1}H NMR ([D$_6$]acetone, 400 MHz): δ = 1.24 (s, 3 H), 1.33 (s, 3 H), 1.34–1.39 (m, 9 H), 1.47 (dd, J_1 = 12.9 Hz, J_2 = 13.0 Hz, 1 H), 1.87 (dd, J_1 = 4.4 Hz, J_2 = 13.1 Hz, 1 H), 2.80–2.89 (m, 4 H), 4.14–4.21 (m, 4 H), 6.60 (d, J = 8.5 Hz, 1 H), 7.24–7.25 (m, 3 H), 7.37 (d, J = 8.5 Hz, 1 H), 7.44 (s, 1 H), 7.79 (d, J = 4.0 Hz, 1 H), 8.03 ppm (d, J = 19.2 Hz, 1 H); HRMS-EI calcd for $C_{26}H_{33}N_2O_3PS$: 484.1949 [M]$^+$; found: 484.1953.

QBCP: ^{1}H NMR ([D$_6$]acetone, 400 MHz): δ = 1.20 (s, 3 H), 1.29 (s, 3 H), 1.31–1.36 (m, 9 H), 1.38 (dd, J_1 = 12.9 Hz, J_2 = 13.0 Hz, 1 H), 1.76 (dd, J_1 = 12.8 Hz, J_2 = 4.2 Hz, 1 H), 2.56–2.64 (m, 1 H), 2.86 (s, 3 H), 4.10–4.14 (m, 4 H), 6.43 (d, J = 8.8 Hz, 1 H), 6.79 (s, 1 H), 6.95 (d, J = 8.7 Hz, 1 H), 7.27–7.34 (m, 2 H), 7.46–7.52 (m, 4 H), 7.79 ppm (d, J = 20 Hz, 1 H); HRMS-EI calcd for $C_{28}H_{35}N_2O_3P$: 478.2385 [M]$^+$; found: 478.2387.

Photophysical properties of **QT**, **QTC**, **QTCP**, and **QBCP** were also investigated by TDDFT calculations, which were performed with the TURBOMOLE program suite.[81] The TDDFT method is widely used to calculate electronic excitation spectra with analytical gradient implementations permitting excited-state geometry optimizations.[8,14,82] Both the geometric structures of ground state and the low-lying electronically excited states were optimized at the B3LYP level with a basis set of triple-ζ valence quality and one set of polarization functions (TZVP).[83,84] Fine quadrature grids of size 4 (both for ground state and excited state) were employed.[85] For the purpose of comparison, the electronic structures of all TMTHQs were also calculated by DFT with B3LYP functional and 6-31G(D,P) basis set by using the Gaussian 03 program package.[86] The transition energies and oscillator strengths were calculated by TDDFT with B3LYP functional and 6-31G(D,P) basis set. The 2D site and 3D cube representations used in the present study have been described in detail elsewhere.[87–92] Briefly, the 3D transition density reveals the orientation and strength of the transition dipole moment, and the 3D charge difference density shows the orientation and results of ICT. The 2D contour plot of the transition density matrix reveals the electron–hole coherence and magnitudes of delocalization (along the diagonal) and exciton (along the off-diagonal).[88]

Acknowledgement

This work was supported by the National Natural Science Foundation of China (Nos. 20373071, 20333050, and 20403020), and NKBRSF (2007CB815202), the Swedish Research Council, and the K & A Wallenberg Foundation.

[1] E. Lippert, W. Lüder, F. Moll, W. Nägele, H. Boos, H. Prigge, I. Seibold-Blankenstein, *Angew. Chem.* **1961**, *73*, 695.

[2] F. F. Huerta, Y. R. S. Laxmi, J. E. Bäckvall, *Org. Lett.* **2000**, *2*, 1037.
[3] L. Boren, B. Martin-Matute, Y. M. Xu, A. Cordova, J. E. Bäckvall, *Chem. Eur. J.* **2006**, *12*, 225.
[4] Z. R. Grabowski, K. Rotkiewicz, W. Rettig, *Chem. Rev.* **2003**, *103*, 3899.
[5] A. Demeter, T. Bérces, K. A. Zachariasse, *J. Phys. Chem. A* **2005**, *109*, 4611.
[6] S. Wilsey, K. N. Houk, A. H. Zewail, *J. Am. Chem. Soc.* **1999**, *121*, 5772.
[7] M. D. Ward, *Chem. Soc. Rev.* **1997**, *26*, 365.
[8] C. J. Jödicke, H. P. Lüthi, *J. Am. Chem. Soc.* **2003**, *125*, 252.
[9] S. O. Kelley, J. K. Barton, *Science* **1999**, *283*, 375.
[10] K. Dahl, R. Biswas, N. Ito, M. Maroncelli, *J. Phys. Chem. B* **2005**, *109*, 1563.
[11] S. P. Argent, H. Adams, T. Riis-Johannessen, J. C. Jeffery, L. P. Harding, O. Mamula, M. D. Ward, *Inorg. Chem.* **2006**, *45*, 3905.
[12] J. Dobkowski, J. Wójcik, W. Koźmiñski, R. Kolos, J. Waluk, J. Michl, *J. Am. Chem. Soc.* **2002**, *124*, 2406.
[13] B. Mennucci, A. Toniolo, J. Tomasi, *J. Am. Chem. Soc.* **2000**, *122*, 10621.
[14] D. Rappoport, F. Furche, *J. Am. Chem. Soc.* **2004**, *126*, 1277.
[15] N. Armaroli, G. Marconi, L. Echegoyen, J. P. Bourgeois, F. Diederich, *Chem. Eur. J.* **2000**, *6*, 1629.
[16] N. Armaroli, G. Accorsi, D. Felder, J. F. Nierengarten, *Chem. Eur. J.* **2002**, *8*, 2314.
[17] F. Lahmani, A. Zehnacker-Rentien, L. H. Coudert, K. A. Zachariasse, *J. Phys. Chem. A* **2003**, *107*, 7364.
[18] J. E. Norton, L. P. Olson, K. N. Houk, *J. Am. Chem. Soc.* **2006**, *128*, 7835.
[19] R. Davis, S. Das, M. George, S. Druzhinin, K. A. Zachariasse, *J. Phys. Chem. A*, **2001**, *105*, 4790.
[20] J.-S. Yang, K.-L. Liau, C.-M. Wang, C.-Y. Hwang, *J. Am. Chem. Soc.* **2004**, *126*, 12325.
[21] J.-S. Yang, S.-Y. Chiou, K.-L. Liau, *J. Am. Chem. Soc.* **2002**, *124*, 2518.
[22] M. N. Paddon-Row, *Aust. J. Chem.* **2003**, *56*, 729.
[23] D. W. Cho, M. Fujitsuka, A. Sugimoto, U. C. Yoon, P. S. Mariano, T. Majima, *J. Phys. Chem. B* **2006**, *110*, 11062.
[24] S. Bahmanyar, K. N. Houk, *J. Am. Chem. Soc.* **2001**, *123*, 11273.
[25] T. Majima, S. Tojo, A. Ishida, S. Takamuku, *J. Phys. Chem.* **1996**, *100*, 13615.
[26] S. Samori, S. Tojo, M. Fujitsuka, H. J. Liang, T. I. Ho, J. S. Yang, T. Majima, *J. Org. Chem.* **2006**, *71*, 8732.
[27] K. A. Jolliffe, T. D. M. Bell, K. P. Ghiggino, S. J. Langford, M. N. Paddon-Row, *Angew. Chem. Int. Ed.* **1998**, *37*, 916.
[28] J. A. Marsden, J. J. Miller, L. D. Shirtcliff, M. M. Haley, *J. Am. Chem. Soc.* **2005**, *127*, 2464.
[29] J. S. Yang, K. L. Liau, C. Y. Hwang, C. M. Wang, *J. Phys. Chem. A* **2006**, *110*, 8003.
[30] J. S. Yang, J. L. Yan, C. Y. Hwang, S. Y. Chiou, K. L. Liau, H. H. G. Tsai, G. H. Lee, S. M. Peng, *J. Am. Chem. Soc.* **2006**, *128*, 14109.
[31] T. D. M. Bell, K. A. Jolliffe, K. P. Ghiggino, A. M. Oliver, M. J. Shephard, S. J. Langford, M. N. Paddon-Row, *J. Am. Chem. Soc.* **2000**, *122*, 10661.
[32] M. N. Paddon-Row, *Adv. Phys. Org. Chem.* **2003**, *38*, 1.
[33] Y. Oseki, M. Fujitsuka, M. Hara, X. C. Cai, Y. Ie, Y. Aso, T. Majima, *J. Phys. Chem. B* **2005**, *109*, 10695.
[34] T. Takada, M. Fujitsuka, T. Majima, *Proc. Natl. Acad. Sci. USA* **2007**, *104*, 11179.
[35] T. Takada, C. Lin, T. Majima, *Angew. Chem.* **2007**, *119*, 6801; *Angew. Chem. Int. Ed.* **2007**, *46*, 6681.
[36] G. M. Davies, S. J. A. Pope, H. Adams, S. Faulkner, M. D. Ward, *Inorg. Chem.* **2005**, *44*, 4656.
[37] W. Z. Alsindi, T. L. Easun, X. Z. Sun, K. L. Ronayne, M. Towrie, J. M. Herrera, M. W. George, M. D. Ward, *Inorg. Chem.* **2007**, *46*, 3696.
[38] A. Hosseini, S. Taylor, G. Accorsi, N. Armaroli, C. A. Reed, P. D. W. Boyd, *J. Am. Chem. Soc.* **2006**, *128*, 15903.
[39] C. E. Cannizzaro, K. N. Houk, *J. Am. Chem. Soc.* **2002**, *124*, 7163.
[40] J. DeChancie, K. N. Houk, *J. Am. Chem. Soc.* **2007**, *129*, 5419.
[41] A. Pigliucci, P. Nikolov, A. Rehaman, L. Gagliardi, C. J. Cramer, E. Vauthey, *J. Phys. Chem. A* **2006**, *110*, 9988.
[42] J. T. Blair, M. R. V. Sahyun, D. K. Sharma, *J Photochem Photobiol A: Chem.* **1994**, *77*, 133.
[43] J. L. Jamison, L. Davenport, B. W. Williams, *Chem. Phys. Lett.* **2006**, *422*, 30.
[44] A. Kohn, C. Hättig, *J. Am. Chem. Soc.* **2004**, *126*, 7399.
[45] C. Hättig, A. Hellweg, A. Kohn, *J. Am. Chem. Soc.* **2006**, *128*, 15672.
[46] Y. Gong, X. M. Guo, S. F. Wang, H. M. Su, A. D. Xia, Q. G. He, F. L. Bai, *J. Phys. Chem. A* **2007**, *111*, 5806.
[47] S. Murali, V. Kharlanov, W. Rettig, A. I. Tolmachev, A. V. Kropachev, *J. Phys. Chem. A* **2005**, *109*, 6420.
[48] A. Chakraborty, S. Kar, N. Guchhait, *Chem. Phys.* **2006**, *324*, 733.
[49] T. Privalov, J. S. M. Samec, J. E. Bäckvall, *Organometallics* **2007**, *26*, 2840.
[50] J. Norinder, J. E. Bäckvall, *Chem. Eur. J.* **2007**, *13*, 4094.
[51] K. Bogar, P. H. Vidal, A. R. A. Leon, J. E. Bäckvall, *Org. Lett.* **2007**, *9*, 3401.
[52] R.-K. Chen, G.-J. Zhao, X.-C. Yang, X. Jiang, J.-F. Liu, H.-N. Tian, Y. Gao, X. Liu, K.-L. Han, M.-T. Sun, L.-C. Sun *J. Mol. Struct.* **2008**, *876*, 102.
[53] M. C. R. Delgado, V. Hernández, J. Casado, J. T. L. Navarrete, J.-M. Raimundo, P. Blanchard, J. Roncali, *Chem. Eur. J.* **2003**, *9*, 3670.
[54] M. Berggren, O. Inganäs, G. Gustafsson, J. Rasmusson, M. R. Andersson, T. Hjertberg, O. Wennerström, *Nature* **1994**, *372*, 444.
[55] M. R. Wasielewski, *Chem. Rev.* **1992**, *92*, 435.
[56] K. Hara, Y. Dan-oh, C. Kasada, O. Yasuyo, A. Shinpo, S. Suga, K. Sayama, H. Arakawa, *Langmuir* **2004**, *20*, 4205.
[57] J. N. Demas, G. A. Grosby, *J. Phys. Chem.* **1971**, *75*, 991.
[58] J. Zhang, Q. Xu, Z. Feng, M. Li, C. Li, *Angew. Chem.* **2008**, *120*, 1790; *Angew. Chem. Int. Ed.* **2008**, *47*, 1766.
[59] P. O. Andersson, T. Gillbro, A. E. Asato, R. S. H. Liu, *J. Lumin.* **1992**, *51*, 11.
[60] G.-J. Zhao, K.-L. Han, *J. Comput. Chem*. **2008**, DOI: 10.1002/jcc.20957.
[61] L.-C. Zhou, G.-J. Zhao, J.-F. Liu, K.-L. Han, Y.-K. Wu, X.-J. Peng, and M.-T. Sun, *J Photochem Photobiol A: Chem.* **2007**, *187*, 305.
[62] G.-J. Zhao, and K.-L. Han, *J. Phys. Chem. A* **2007**, *111*, 2469.
[63] G.-J. Zhao, J.-Y. Liu, L.-C. Zhou, K.-L. Han, *J. Phys. Chem. B* **2007**, *111*, 8940.
[64] G.-J. Zhao, K.-L. Han, *J. Phys. Chem. A* **2007**, *111*, 9218.
[65] G.-J. Zhao, K.-L. Han, *J. Chem. Phys.* **2007**, *127*, 024306.
[66] G.-J. Zhao, K.-L. Han, Y.-B. Lei, and Y.-S. Dou, *J. Chem. Phys.* **2007**, *127*, 094307.
[67] G.-J. Zhao, and K.-L. Han, *Biophys. J.* **2008**, *94*, 38.
[68] N. Mataga, Y. Kaifu, M. Koizumi, *Bull. Chem. Soc. Jpn.* **1956**, *29*, 465.
[69] W. Liptay in *Excited States, Vol. 1* (Ed.: E. C. Lim), Academic Press, New York, **1974**, p. 129.
[70] S. Sumalekshmy, K. R. Gopidas, *J. Phys. Chem. B* **2004**, *108*, 3705.
[71] A. R. Katritzky, D.-W. Zhu, K. S. Schanze, *J. Phys. Chem.* **1991**, *95*, 5737.
[72] T.-Y. Chu, Y.-S. Wu, J.-F. Chen, C. H. Chen, *Chem. Phys. Lett.* **2005**, *404*, 121.
[73] I. Kondov, H.-B. Wang, M. Thoss, *Int. J. Quantum Chem.* **2006**, *106*, 1291.
[74] L.-H. Ma, Z.-B. Chen, Y.-B. Jiang, *Chem. Phys. Lett.* **2003**, *372*, 104.
[75] M. T. Sun, *Chem. Phys.* **2006**, *320*, 155.
[76] C. Yang, L. M. Fu, Y. Wang, J. P. Zhang, W. T. Wong, X. C. Ai, Y. F. Qiao, B. S. Zou, L. L. Gui, *Angew. Chem.* **2004**, *116*, 5230; *Angew. Chem. Int. Ed.* **2004**, *43*, 5120.
[77] C. Yang, L. M. Fu, Y. Wang, J. P. Zhang, W. T. Wong, X. C. Ai, Y. F. Qiao, B. S. Zou, L. L. Gui, *Angew. Chem.* **2004**, *116*, 5120; *Angew. Chem. Int. Ed.* **2004**, *43*, 5010.
[78] M. T. Sun, Y. H. Chen, P. Song, F. C. Ma, *Chem. Phys. Lett.* **2005**, *413*, 110.

[79] H. Oka, T. Tamura, Y. Miura, T. Yoshio, *J. Mater. Chem.* **2001**, *11*, 1364.
[80] P. J. Scheuer, W. I. Kimoto, K. Ohinata, *J. Am. Chem. Soc.* **1953**, *75*, 3029.
[81] R. Ahlrichs, M. Bär, H. Horn, C. Kölmel, *Chem. Phys. Lett.* **1989**, *162*, 165.
[82] C. Jamorski, J. B. Foresman, C. Thilgen, H. P. Lüthi, *J. Chem. Phys.* **2002**, *116*, 8716.
[83] A. D. Becke, *J. Chem. Phys.* **1993**, *98*, 5648.
[84] A. Schäfer, C. Huber, R. Ahlrichs, *J. Chem. Phys.* **1994**, *100*, 5829.
[85] O. Treutler, R. Ahlrichs, *J. Chem. Phys.* **1995**, *102*, 346.
[86] Gaussian 03, revision C.02, M. J. Frisch, G. W. Trucks, H. B. Schlegel, G. E. Scuseria, M. A. Robb, J. R. Cheeseman, J. A., Jr., Montgomery, T. Vreven, K. N. Kudin, J. C. Burant, J. M. Millam, S. S. Iyengar, J. Tomasi, V. Barone, B. Mennucci, M. Cossi, G. Scalmani, N. Rega, G. A. Petersson, H. Nakatsuji, M. Hada, M. Ehara, K. Toyota, R. Fukuda, J. Hasegawa, M. Ishida, T. Nakajima, Y. Honda, O. Kitao, H. Nakai, M. Klene, X. Li, J. E. Knox, H. P. Hratchian, J. B. Cross, C. Adamo, J. Jaramillo, R. Gomperts, R. E. Stratmann, O. Yazyev, A. J. Austin, R. Cammi, C. Pomelli, J. W. Ochterski, P. Y. Ayala, K. Morokuma, G. A. Voth, P. Salvador, J. J. Dannenberg, V. G. Zakrzewski, S. Dapprich, A. D. Daniels, M. C. Strain, O. Farkas, D. K. Malick, A. D. Rabuck, K. Raghavachari, J. B. Foresman, J. V. Ortiz, Q. Cui, A. G. Baboul, S. Clifford, J. Cioslowski, B. B. Stefanov, G. Liu, A. Liashenko, P. Piskorz, I. Komaromi, R. L. Martin, D. J. Fox, T. Keith, M. A. Al-Laham, C. Y. Peng, A. Nanayakkara, M. Challacombe, P. M. W. Gill, B. Johnson, W. Chen, M. W. Wong, C. Gonzalez, J. A. Pople, Gaussian, Inc., Pittsburgh, PA, **2003**.
[87] S. Mukamel, S. Tretiak, T. Wagersreiter, V. Chernyak, *Science* **1997**, *277*, 781.
[88] S. Tretiak, S. Mukamel, *Chem. Rev.* **2002**, *102*, 3171.
[89] G.-J. Zhao, Y.-H. Liu, K.-L. Han, and Y. Dou, *Chem. Phys. Lett.* **2008**, *453*, 29.
[90] N. K. Persson, M. T. Sun, P. Kellberg, T. Pullerits, O. Inganäs, *J. Chem. Phys.* **2005**, *123*, 204718.
[91] B. P. Krueger, G. D. Scholes, G. R. Fleming, *J. Phys. Chem. B* **1998**, *102*, 5378.
[92] W. J. D. Beenken, T. Pullerits, *J. Phys. Chem. B* **2004**, *108*, 6164.

Received: November 27, 2007
Revised: April 24, 2008
Published online: June 24, 2008